

Light Scattering by Homogeneous Axisymmetric Particles for PDA Calculations to Measure Both Axes of Spheroidal Particles

Adrian Doicu*, Thomas Wriedt*, Klaus Bauckhage**

(Received: 15 July 1996; resubmitted: 30 September 1996)

Abstract

Mathematical tools are provided for the computation of the scattered field produced by a non-spherical particle moving through the measurement volume of a phase Doppler anemometer. The Doppler signal is modeled by using the rigorous extended boundary condition method and an approximate ray

theory. The region of applicability of ray theory is discussed. In particular, a pure refraction model is considered for large particles. It is shown that under some circumstances the phase Doppler technique may be used for sizing of spheroidal particles.

1 Introduction

Phase Doppler anemometry (PDA) is a method used to determine the size and velocity of spherical particles in different engineering processes, e.g. spray drying and ultrasonic atomization. The design of a phase Doppler system includes simulations based on Mie theory, which describes the scattering of a plane wave by a spherical particle. Usually, there are non-spherical particles to be measured which are assumed spherical-like fluid particles which may be deformed by oscillation effects in the process of their development, or by interaction of several particles, turbulences or aerodynamic resistance. For example, the instantaneous deformation of the shape of an oscillating droplet can be described by an infinite series of surface spherical harmonics, where each term corresponds to one independent natural oscillation mode [1]. Furthermore, in three-dimensional flows the drop deforms to spherical cap shapes at low Reynolds numbers and becomes ellipsoidal as the Reynolds number increases [2]. It is thus justified to adapt the theories of light scattering by homogenous non-spherical particles for PDA calculations.

Many techniques have been developed for analyzing scattering and diffraction problems involving dielectric obstacles. At present the extended boundary condition method (EBCM) is one of the most efficient and powerful tools for rigorously computing non-spherical scattering based on directly solving Maxwell's equations [3, 4]. The main advantages of the EBCM are high and easily controllable numerical accuracy, superior numerical efficiency and analyticity of the mathematical formulation.

However, for large size parameters, the approximate methods for calculating the far-zone scattered intensity have superior computational efficiency to the rigorous methods. One of these approximate methods is the ray theory. The ray theory, accounting for diffraction,

reflection and transmission, gives a good approximation of the far-zone intensity in the forward scattering hemisphere [5–7]. The higher computational speed makes it economically viable to compute the amplitude and phase of the scattered light over a fine grid on the receiver aperture.

The aim of this paper is to model the phase Doppler signal by using the rigorous EBCM and the approximate ray theory. The general concern is the range of applicability of the ray theory and, in particular, of a simplified pure refraction model. The application of these theoretical models to the measurement of spheroidal particles with a fixed orientation by a phase Doppler system is also investigated. We note here that the assumption that the spheroids have a fixed orientation represents the first step in the investigation of the complex problem of non-spherical particles arbitrarily positioned. The non-spherical water droplets produced by a droplet generator or the fluid particles formed in a flow under shear gradient conditions can be considered, under some circumstances, as spheroids with a fixed orientation.

2 Scattering Theories

2.1 Notations

The scattering geometry is presented in Figure 1 for the general case of Gaussian beam incidence.

We consider an electromagnetic wave of wavelength λ and propagation number k and define the original beam coordinate system OXYZ such that the center of the Gaussian beam waist is located at the point O. The waist radius of the Gaussian beam is w_0 and the direction of propagation is along the Z axis. The polarization direction of the incident electric field makes an angle α_p with the X axis. An axisymmetric particle is illuminated by the Gaussian beam. The center of the scatterer is located at the point o of a Cartesian coordinate system $oxyz$, which is called by convention the particle location system. The particle is oriented with the symmetry axis in the (β, α) direction referenced to the beam coordinate system. We denote by (x_0, y_0, z_0) the coordinates of the particle center in the beam frame.

* Dr.-Ing. A. Doicu, Dr.-Ing. T. Wriedt, Institut für Werkstofftechnik, Badgasteinerstraße 3, D-28359 Bremen (Germany).

** Prof. Dr.-Ing. K. Bauckhage, Fachgebiet Verfahrenstechnik, Universität Bremen, Badgasteinerstraße 3, D-28359 Bremen (Germany).

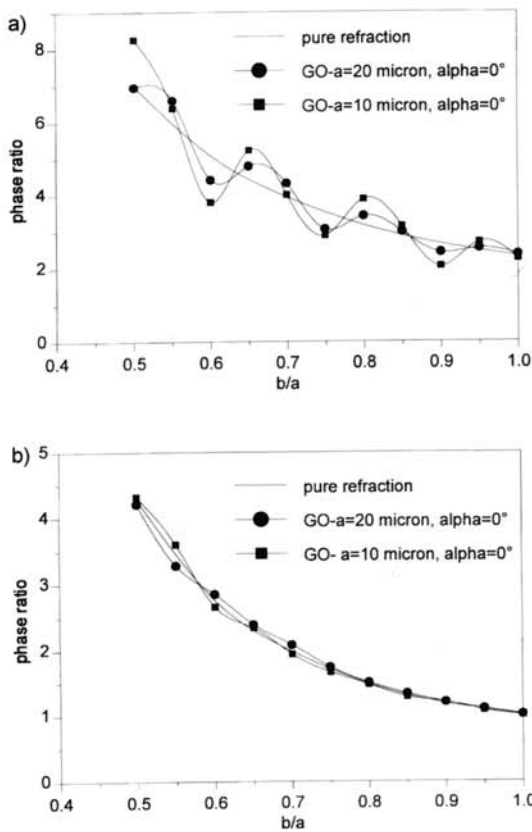


Fig. 11: Phase ratio computed in the pure refraction model and the geometric optics model as a function of the particle eccentricity. (a) Optical system A; (b) optical system B.

owing to the symmetry of the optical configuration, for a fixed value of the orientation angle α in the range $0-30^\circ$ one can invert the ratio of the signals to obtain the same maximal sensitivity as for the complementary domain.

One would expect that the computed phase ratio in the geometrical optics model will exhibit fluctuations even if the refraction mechanism is dominant. In a given range for the semi-major dimension a the smoothness of the response curve will be used as a criterion for selection. In Figure 11 we have plotted the computed phase ratio in the geometrical optics model for $a = 20$ and $10 \mu\text{m}$. The relationship between phase ratio and particle eccentricity shows substantial fluctuations in case A. The explanation lies in the fact that even for spherical particles the phase versus size calibration of the planar system is not linear. With increasing spheroid-size parameter the fluctuations are suppressed. From the above analysis, we conclude that the optical system B may be used, formally, for the recognition of spheroidal particles with the semi-major axis in the range $10-20 \mu\text{m}$.

5 Conclusions

In order to examine the behavior of the signal phase in a phase Doppler system, fundamentals of light scattering from nonspherical particles in the intersection of two laser beams have been discussed. Mathematical tools based on the rigorous extended boundary condition method and the approximate ray theory have been presented. In addition, a pure refraction model has been examined. The case of spheroidal particles has been investigated numerically. It has been shown that for particles with spheroid-size parameters larger than 25 and for scattering angles smaller

than the critical value at which total internal reflection occurs, the results obtained by the geometrical optics model agree, within certain bounds, with those obtained by using the rigorous model. The application of these mathematical tools to the measurement of spheroidal particles with a fixed orientation has also been considered. It has been shown that, from a theoretical point of view, the size parameters of a spheroidal particle can be measured using an optical configuration which combines two standard Doppler systems.

6 Acknowledgements

The authors are grateful to the DFG (German Research Society) for providing financial support for this work.

7 Symbols and Abbreviations

a, b	semi-major and semi-minor axes of a spheroid
(a_{nm}, b_{mn})	incident field coefficients
C	boundary of the projected particle surface on to a plane normal to the incident vector
C_{mn}, D_{mn}	normalization constants
e	particle eccentricity
$(\bar{e}_\Phi, \bar{e}_\Psi)$	unit vectors of the (Φ_s, Ψ_s) direction
E_0	incident electric field strength
$\bar{E}_{sca}(\bar{r})$	scattered electric field
$f(e), F(e)$	functions of the particle eccentricity
(f_{mn}, g_{mn})	scattered field coefficients
k	propagation constant
K_{mn}	correction factor
L_{AB}	distance of travel of the ray inside the particle
L_{trans}	optical path length of the transmitted ray
m	real part of the refractive index
$(\bar{M}_{mn}^3, \bar{N}_{mn}^3)$	radiating spherical vector wavefunctions
n	number of caustic participations
\bar{n}_A, \bar{n}_B	unit vectors normal to the surface at the points A and B
\bar{n}_{AB}	unit vector of the transmitted ray inside the particle
\bar{n}_i	unit vector of the incident ray in the particle location system
\bar{n}_s	unit vector of the scattered ray (transmitted or reflected)
$r_p(\theta)$	particle surface representation in spherical coordinates
r_s, r_p	Fresnel coefficients for reflection
$R(\bar{u}, \bar{v})$	plane rotation matrix
$R_{mn}^m(\alpha, \beta, \gamma)$	rotation matrix for spherical vector wavefunctions
(\bar{s}_i, \bar{p}_i)	unit vectors of the incident ray in the s and p polarization directions in the case of specular reflection
$(\bar{s}_{iA(B)}, \bar{p}_{iA(B)})$	unit vectors in the s and p polarization directions for the incident ray at the A and B interfaces
(\bar{s}_r, \bar{p}_r)	unit vectors of the reflected ray in the s and p polarization directions
$(\bar{s}_{tA(B)}, \bar{p}_{tA(B)})$	unit vectors in the s and p polarization directions for the transmitted ray at the A and B interfaces
$S(\Phi_s, \Psi_s)$	magnitude of the electric field contribution obtained by ignoring the Fresnel coefficients at the particle surface

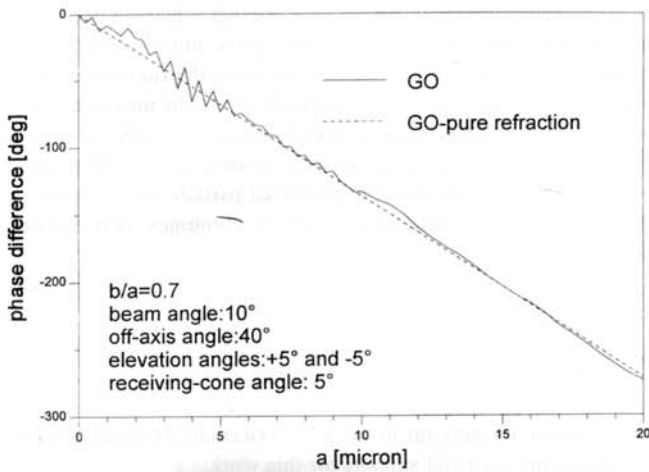


Fig. 7: Signal phase versus the semi-major axis of the spheroid for a given eccentricity $e = 0.7$ and a given orientation $\alpha = 90^\circ, \beta = 90^\circ$.

The flow direction is along the Y axis. The parameters of the optical configurations are given in Table 1. We restrict our analysis to the measurement of prolate particles with e ranging from 0.5 to 1. The angle between the Z axis and the particle symmetry axis is set to 90° . The dependence of the phase ratio, computed in the pure refraction model, on the particle eccentricity is shown in Figure 10 for different values of the orientation angle α . The optical system A would be effective in recognizing particle eccentricities if the azimuthal angle α is fixed in the range $60-90^\circ$. The best sensitivity is achieved if the particle symmetry axis is along the Y axis, also for $\alpha = 90^\circ$. The optical system B has the same sensitivity with respect to the particle eccentricity in the range $60-90^\circ$. However,

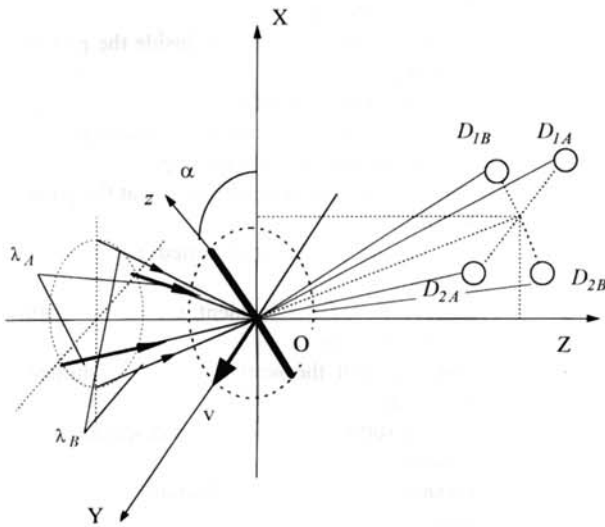


Fig. 8: Optical layout of system A, dual-mode PDA.

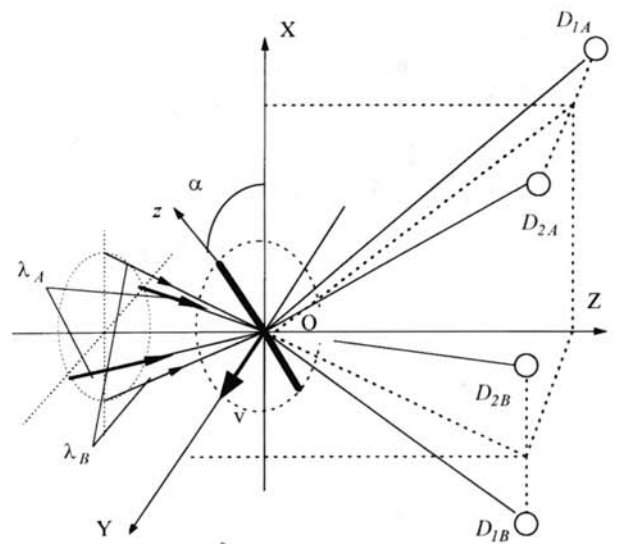


Fig. 9: Optical layout of system B.

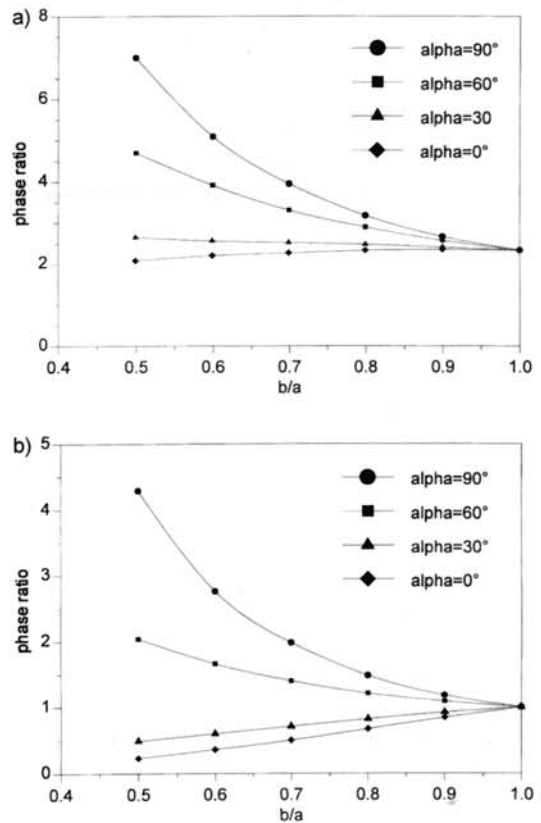


Fig. 10: Phase ratio computed in the pure refraction model as a function of the particle eccentricity. (a) Optical system A; (b) optical system B.

Table 1: Parameters of the optical systems A and B.

Optical parameter	System A		System B	
	Detectors A	Detectors B	Detectors A	Detectors B
beam angle	5°	6°	5°	5°
off-axis angle	40°	0°	40°	40°
elevation angle	-5° and 5°	45° and 35°	-5° and 5°	-5° and 5°
receiving-cone angle	5°	5°	5°	5°

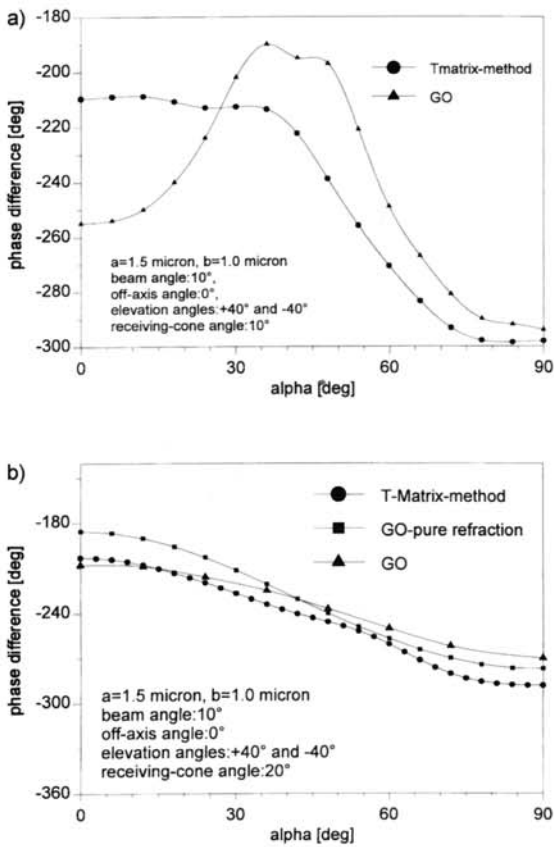


Fig. 4: Signal phase of a spheroidal particle with $a = 1.5 \mu\text{m}$ and $b = 1.0 \mu\text{m}$ as a function of the azimuthal orientation angle α . (a) Receiving-cone angle 10° ; (b) receiving-cone angle 20° .

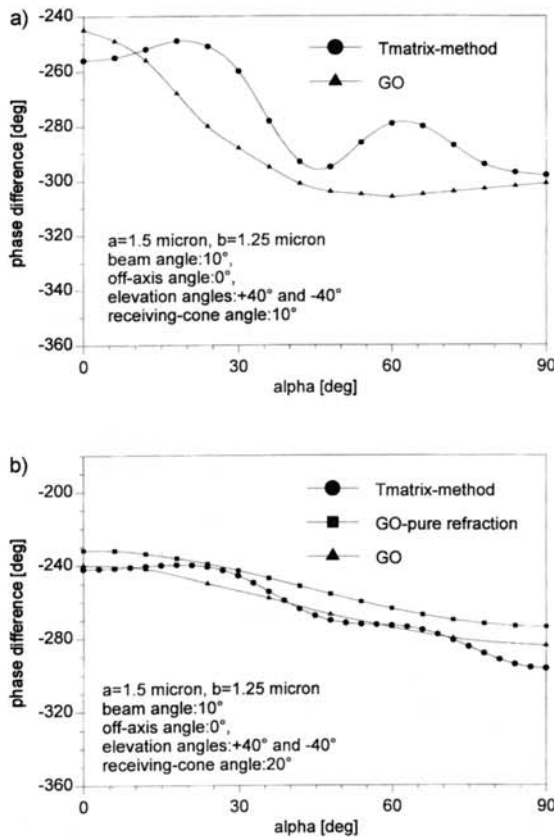


Fig. 5: Signal phase of a spheroidal particle with $a = 1.5 \mu\text{m}$ and $b = 1.25 \mu\text{m}$ as a function of the azimuthal orientation angle α . (a) Receiving-cone angle 10° ; (b) receiving-cone angle 20° .

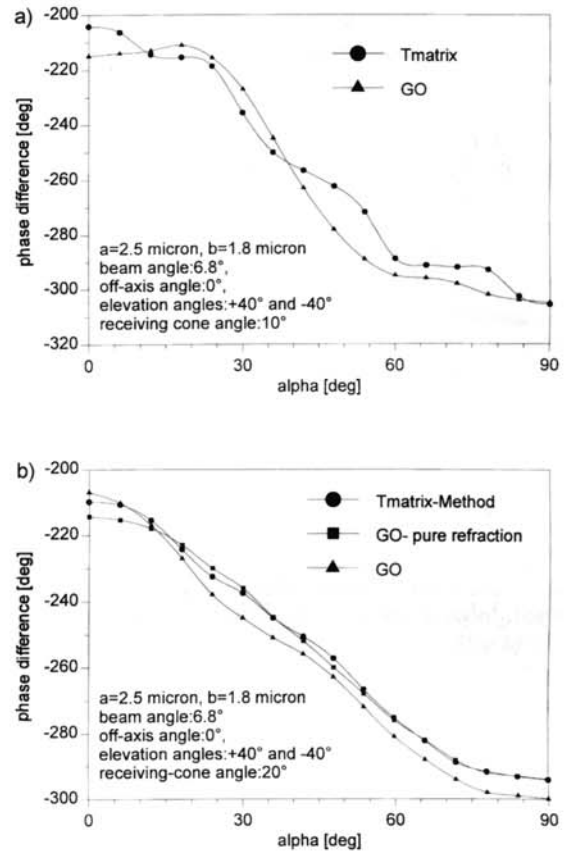


Fig. 6: Signal phase of a spheroidal particle with $a = 2.5 \mu\text{m}$ and $b = 1.8 \mu\text{m}$ as a function of the azimuthal orientation angle α . (a) Receiving-cone angle 10° ; (b) receiving-cone angle 20° .

4 Size Measurements of Spheroidal Particles

Under certain conditions, a phase Doppler system may be employed for size measurements of spheroidal particles. Examination of Eq. (11) shows that the phase signals ϕ computed by using the pure refraction model may be written as $\phi = af(e)$, where f is a function of the particle eccentricity $e = b/a$. The explanation lies in the fact that for a class of parallel surfaces the ratio ϕ/a is constant. The linear relationship between the phase signals and the semi-major axis of the spheroid, for given particle eccentricity and orientation, can also be found by using the geometrical optics model. The data plotted in Figure 7 show the agreement between the geometrical optics model and the pure refraction model for large spheroid-size parameters. The optical configuration corresponds to a standard PDA with the following parameters: beam intersection angle 10° , off-axis angle 40° , elevation angles 5° and -5° and receiving-cone angle 5° . If refraction-dominated signals are collected at two different off-axis angles, the ratio of these phase signals depends only on the particle eccentricity, i.e. $\phi_A/\phi_B = F(e)$. If the curve $F(e)$ is monotonic then the particle eccentricity can be obtained from the ratio of the phase signals.

For size measurements of spheroidal particles we analyze two optical configurations, A and B: (A) a dual mode PDA which essentially combines a standard PDA system with a planar PDA in a two-velocity component system [15], as shown in Figure 8, and (B) an optical system which consists of two separate transmitters having different laser wavelengths and two separate receivers placed symmetrically about the XZ and YZ plane. This system combines two standard PDA systems as illustrated in Figure 9.

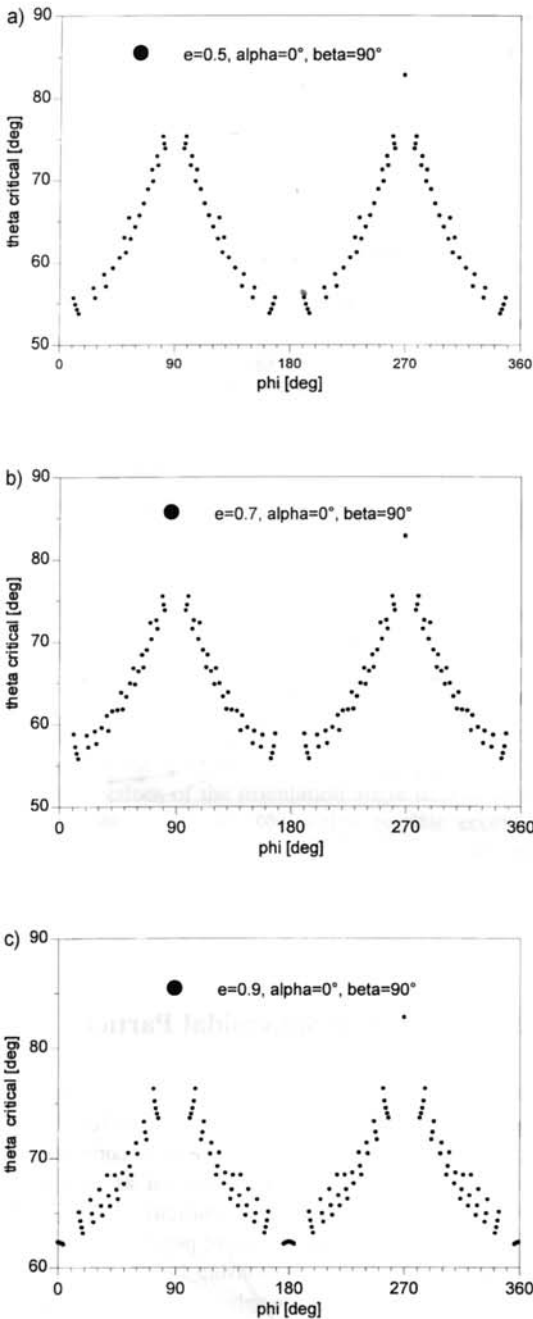


Fig. 2: Critical value of the scattering angle $\Phi_{critical}$ as a function of the azimuthal angle Ψ for a given orientation of the particle and for different values of the spheroid eccentricity.

particles require a value of the scattering angle in the vicinity of the Brewster angle [13], or a large beam intersection angle [14]. In this case the transmission in the vicinity of the critical angle for total internal reflection occurs and the ray theory is not valid. However, the response curves for the planar system have less oscillations than those for the standard system.

The signal phase of a planar optical arrangement with a beam intersection angle of 10° and elevation angles of 40° and -40° were calculated for spherical particles using the Lorenz-Mie theory. The response curves are shown in Figure 3. The receiving-cone angles are taken to be 10° and 20° for Figure 3a and b, respectively. A relatively monotonic phase-diameter relationship can be observed for the optical configuration with the receiving-cone angle of 20° in the particle diameter range 2-3 μm .

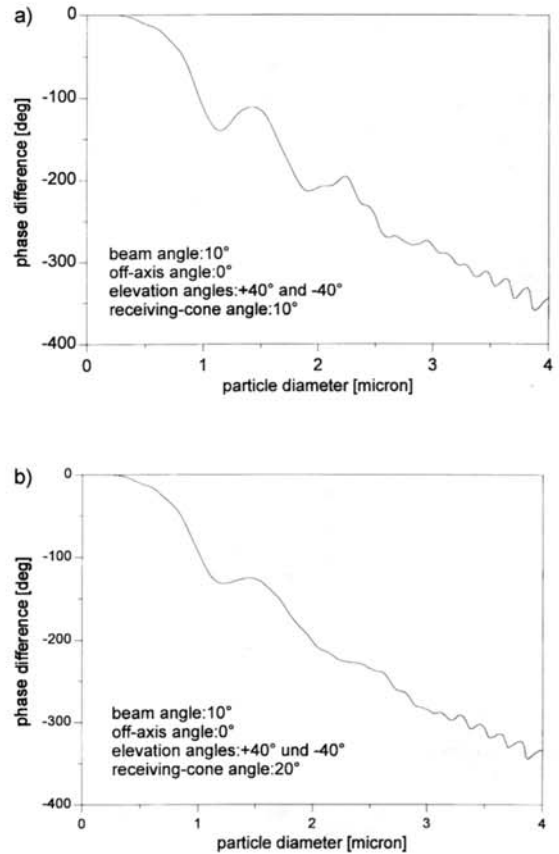


Fig. 3: Response curves for spherical particles in a planar optical system. (a) Receiving-cone angle 10° ; (b) receiving-cone angle 20° .

The signal phases of a spheroidal particle with $a = 1.5 \mu\text{m}$ and $b = 1.0 \mu\text{m}$ as a function of the azimuthal orientation angle α are shown in Figure 4. The Euler angle β is 90° . The same curves are plotted in Figure 5 for a spheroidal particle with $a = 1.5 \mu\text{m}$ and $b = 1.25 \mu\text{m}$. There are significant deviations between the signal phases computed by using the extended boundary condition method and the ray theory for a value of the receiving-cone angle of 10° . However, for the optical configuration with a receiving-cone angle of 20° , the relative errors are about 7% for the geometrical optics model and less than 10% for the pure refraction model. The maximum relative error is of the same order as the relative phase error of a spherical particle having the size parameter in the range from kb to ka . The large deviations of the signal phases show that the ray theory cannot be applied for small values of the spheroid-size parameter. However, the large aperture suppresses the deviations of the scattered fields by integration over a large region.

An optical configuration with a beam intersection angle of 6.8° and elevation angles of 40° and -40° is considered. The data presented in Figure 6 are for a spheroidal particle with $a = 2.5 \mu\text{m}$ and $b = 1.8 \mu\text{m}$. The values of the receiving-cone angles are the same as in the above examples. In this case the relative error is about 6% for the optical arrangement with the receiving-cone angle of 10° , and about 4% for the optical system with the receiving-cone angle of 20° . As expected, the phase error decreases as the spheroid-size parameter increases.

From the above numerical results, one may conclude that the geometrical optics model can be used to compute the response of a phase Doppler system for particles with spheroid-size parameter larger than 25, scattering angles smaller than the critical value where total internal reflection occurs and large receiving-cone angle.

(ii) The phase of the reflected ray is

$$\delta_{ref} = k[\bar{r}_A(\bar{n}_i - \bar{n}_s)] - (n+1)\frac{\pi}{2}. \quad (19)$$

For a spheroidal particle $n = 0$, and therefore the reflected phase shift for an arbitrary spheroid orientation in Eq. (19) is $-\pi/2$ [5].

(iii) The polarization vector of the reflected ray is written in the beam coordinate system as

$$\bar{e}_{ref} = \varepsilon_{\Phi}^{ref} \bar{e}_{\Phi} + \varepsilon_{\Psi}^{ref} \bar{e}_{\Psi} \quad (20)$$

where the following successive transformations are considered:

$$\begin{aligned} \{\varepsilon_{s,i}; \varepsilon_{p,i}\}^T &= R(\bar{e}_X, \bar{s}_i) \{\cos\alpha_p, \sin\alpha_p\}^T \\ \varepsilon_{s,r} &= \varepsilon_{s,i} r_s, \quad \varepsilon_{p,r} = \varepsilon_{p,i} r_p \\ \{\varepsilon_{\Phi}^{ref}; \varepsilon_{\Psi}^{ref}\}^T &= R(\bar{s}_r, \bar{e}_{\Phi}) \{\varepsilon_{s,r}; \varepsilon_{p,r}\}^T. \end{aligned} \quad (21)$$

We denote by r_s and r_p the Fresnel coefficients for reflection and by (\bar{s}_i, \bar{p}_i) and (\bar{s}_r, \bar{p}_r) the unit vectors in the s and p polarization directions for the reflected electric field [5].

2.3.3 Diffracted Electric Field

The magnitude of the diffracted electric field can be computed if we are able to evaluate the projection of the arbitrarily oriented particle surface on to a plane normal to the incident vector. For this purpose we choose an auxiliary coordinate system $ox_1y_1z_1$, rotated with respect to the OXYZ system by the angle α about the Z axis. A parametric representation of the curve C , which represents the boundary of the projected particle surface on to the ox_1y_1 plane, is given by

$$\begin{aligned} x_1(\theta) &= r_p(\theta) \sin\theta \frac{\cos\Sigma \cos^2\beta}{\sin\Sigma \sin\beta} + r_p(\theta) \cos\theta \sin\beta \\ y_1(\theta) &= r_p(\theta) \sin\theta \sqrt{\frac{\sin^2\Sigma \sin^2\beta - \cos^2\Sigma \cos^2\beta}{\sin\Sigma \sin\beta}}. \end{aligned} \quad (22)$$

where $\theta = \arctan(\bar{r}_p/\bar{r}_p) = \Sigma$.

For a spheroidal particle the curve C is the ellipse with the semi-major axis $A = (a^2 \sin^2\beta + b^2 \cos^2\beta)^{0.5}$ and the semi-minor axis $B = b$.

(i) The curve C serves as the boundary of the effective aperture for Fraunhofer diffraction by the particle:

$$\begin{aligned} S_{dif}(\Phi_s, \Psi_s) &= \frac{k^2}{2\pi} \int_{S_a} e^{-ik[x_1 \sin\Phi_s \cos(\Psi_s - \alpha) + y_1 \sin\Phi_s \sin(\Psi_s - \alpha)]} dx_1 dy_1, \\ C &= \partial S_a. \end{aligned} \quad (23)$$

(ii) The phase of the diffracted electric field is $\delta_{dif} = 0$.

(iii) The polarization vector of the diffracted ray is referenced in the particle coordinate system with respect to the polarization directions \bar{s}_r and \bar{p}_r of the reflected ray and is given by

$$\bar{e}_{dif} = \varepsilon_{\Phi}^{dif} \bar{e}_{\Phi} + \varepsilon_{\Psi}^{dif} \bar{e}_{\Psi} = \varepsilon_{s,i} \bar{s}_r + \varepsilon_{p,i} \bar{p}_r \quad (24)$$

where $\varepsilon_{s,i}$ and $\varepsilon_{p,i}$ are given in Eq. (21) and $\{\varepsilon_{\Phi}^{dif}; \varepsilon_{\Psi}^{dif}\}^T = R(\bar{s}_r, \bar{e}_{\Phi}) \{\varepsilon_{s,i}; \varepsilon_{p,i}\}^T$.

In PDA, we are interested in computing the scattered electric field in a given direction (Φ_s, Ψ_s) , or in a small solid angle around a

given direction (Φ_s, Ψ_s) . For a spheroidal particle, the diffracted and the reflected fields are directly expressible in terms of Φ_s and Ψ_s . However, this is not possible for the transmitted electric field because Eqs. (6) and (7) cannot be analytically inverted to obtain (θ_A, φ_A) as functions of (Φ_s, Ψ_s) or (θ_s, φ_s) . This implies that the inversion must be performed numerically. For this purpose we generate a dense grid of θ_A^* and φ_A^* . Then, for each pair $(\theta_A^*, \varphi_A^*)$ we compute the unit vector of the ray which is transmitted out of the particle \bar{n}_s^* and obtain (θ_A, φ_A) as solutions of the minimum problem $(\theta_A, \varphi_A) = \min_{(\theta_A^*, \varphi_A^*)} |\bar{n}_s^* - \bar{n}_s|$. We numerically perform the derivatives in Eq. (9) and compute the magnitude, the phase and the polarization vector of transmitted, reflected and diffracted fields.

We note that for an arbitrarily axisymmetric particle the angular coordinate of the incident ray θ_A corresponding to the reflected electric field must also be numerically computed as a solution of the nonlinear Eq. (15).

There are some limitations of the ray theory, which are discussed below.

- (i) The transmission in the vicinity of the critical angle for total internal reflection is not taken into account. For a spherical water droplet ($m = 1.334$) the critical value of the scattering angle where total internal reflection occurs is $\Phi_{critical} = 82^\circ$. For a spheroidal particle $\Phi_{critical}$ depends on the orientation of the particle and the spheroid eccentricity. The variations of the critical value of the scattering angle with the azimuthal angle Ψ are presented in Figure 2, for a given orientation of the particle ($\alpha = 0^\circ, \beta = 90^\circ$) and for different values of the spheroid eccentricity. The plotted data show that $\Phi_{critical}$ is about 55° for $b/a = 0.5$ and $\Psi = 0^\circ$ or $\Psi = 180^\circ$. For $\Psi = 90^\circ$ or $\Psi = 270^\circ$, $\Phi_{critical} = 82^\circ$ as expected. The neglect of the transmission in the vicinity of the critical angle for total internal reflection causes ray theory to be inaccurate for scattering angles $\Phi > \Phi_{critical}$.
- (ii) The evaluation of the phase of the transmitted and reflected rays requires a complete description of the caustic structure because there is an additional shift of $\pi/2$ in the phase of geometric light each time it participates in an interior caustic, a near-zone caustic or a far-zone caustic. This problem must be solved for each surface geometry and particle orientation. More details about the caustic structure for reflection and transmission are given elsewhere [6, 11].
- (iii) The problem of implementing a Gaussian beam approximation into a geometrical optics model is currently under study. We have reservations about considering only the variation in the amplitude of the incident wave and the assumption that the incident wavefronts are plane. A possible solution to this problem can be given if one uses the plane wave spectrum representation of Gaussian beams.

3 Theoretical Simulations

In this section we compare the response of a phase Doppler system computed by using the rigorous extended boundary condition method and the approximate geometrical optics model. Additionally, the signal phase is computed for the case of dominant refraction by using a pure refraction model.

The comparison will be performed for small particles. For this purpose we consider a planar optical system [12]. The planar layout allows one to obtain large phase shifts from small particles while maintaining small angles between the laser beams. Other optical configurations dedicated to the measurement of small

The algorithm for deriving the far-zone electric field for diffraction, reflection and transmission is summarized below.

2.3.1 Transmitted Electric Field

Each incident ray is parametrized by (θ_A, φ_A) , which represent the spherical angular coordinates of point A laying on the particle surface struck by the incident light rays. If \bar{n}_i is the unit vector of the incident ray written in the particle coordinate system, i.e. $\bar{n}_i(-\sin\beta, 0, \cos\beta)$, the condition that the point A lies on the lit side of the particle is $-\bar{n}_i \cdot \bar{n}_A \geq 0$, where \bar{n}_A is the unit normal to the surface at the point A . For the rays that graze the edge of the particle $\bar{n}_i \cdot \bar{n}_A = 0$.

In order to evaluate the quantities of the transmitted electric field, the scattering angles (Φ_s, Ψ_s) or (θ_s, φ_s) must be related to (θ_A, φ_A) . For a given entrance point (θ_A, φ_A) we compute the unit vector of the transmitted ray inside the particle as

$$\bar{n}_{AB} = \left[-\frac{1}{m} \bar{n}_i \cdot \bar{n}_A - \sqrt{1 - \frac{1}{m^2} + \frac{(\bar{n}_i \cdot \bar{n}_A)^2}{m^2}} \right] \bar{n}_A + \frac{1}{m} \bar{n}_i. \quad (6)$$

The unit vector of the ray which is transmitted by the particle $\bar{n}_s(\sin\theta_s \cos\varphi_s, \sin\theta_s \sin\varphi_s, \cos\theta_s)$ is given by

$$\bar{n}_s = \left[\sqrt{1 - m^2[1 - (\bar{n}_B \cdot \bar{n}_{AB})^2]} - m(\bar{n}_B \cdot \bar{n}_{AB}) \right] \bar{n}_B + m\bar{n}_{AB}. \quad (7)$$

In Eq. (7), B is the point where the transmitted ray exits the particle, $B = \Delta_{AB} \cap S_p$, with $\Delta_{AB} = \{\bar{r}/\bar{r} - \bar{r}_A = \mu\bar{n}_{AB}\}$ and \bar{n}_B is the unit normal to the surface at this point. Thus, for given coordinates (θ_A, φ_A) of the incident ray, its scattering angles (θ_s, φ_s) are obtained by combining Eqs. (6) and (7). We note that if $m^2[1 - (\bar{n}_B \cdot \bar{n}_{AB})^2] > 1$, total internal reflection occurs. This situation is not taken into account in our analysis.

- (i) The magnitude of the transmitted electric field, sometimes called the gain or divergence, can be obtained by considering the energy conservation, as

$$S_{trans}(\Phi_s, \Psi_s) = \left(\frac{k^2 r_A \sqrt{r_A^2 + r_A^2 \sin^2 \theta_A \cos^2 \Omega}}{\sin \Phi_s \frac{\partial(\Phi_s, \Psi_s)}{\partial(\theta_A, \varphi_A)}} \right)^{0.5} \quad (8)$$

where $r_A = r_p(\theta_A)$, $r_A = dr_p(\theta_A)/d\theta$, $\cos \Omega = -\bar{n}_i \cdot \bar{n}_A$ and

$$\frac{\partial(\Phi_s, \Psi_s)}{\partial(\theta_A, \varphi_A)} = \begin{vmatrix} \frac{\partial \Phi_s}{\partial \theta_A} & \frac{\partial \Phi_s}{\partial \varphi_A} \\ \frac{\partial \Psi_s}{\partial \theta_A} & \frac{\partial \Psi_s}{\partial \varphi_A} \end{vmatrix}. \quad (9)$$

- (ii) The phase of the transmitted ray is given by

$$\delta(\Phi_s, \Psi_s) = kL_{trans} - (n + 1) \frac{\pi}{2} \quad (10)$$

where n is an integer indicating the number of caustic participations, and

$$L_{trans} = \bar{r}_A \bar{n}_i - \bar{r}_B \bar{n}_s + mL_{AB} \quad (11)$$

where L_{AB} is the distance of travel of the ray inside the particle. For a spheroidal particle with spheroid eccentricity satisfying $a^2/b^2 < m/(m-1)$, $n = 2$, therefore the transmitted phase shift for an arbitrary spheroid orientation in Eq. (11) is $-3\pi/2$ [6].

- (iii) The polarization vector of the transmitted ray is written in the beam coordinate system with respect to the unit vectors \bar{e}_Φ and \bar{e}_Ψ of the (Φ_s, Ψ_s) direction as

$$\bar{e}_{trans} = \varepsilon_\Phi^{trans} \bar{e}_\Phi + \varepsilon_\Psi^{trans} \bar{e}_\Psi \quad (12)$$

where the following transformations are considered at the entrance interface A and the exit interface B :

$$\begin{aligned} \{\varepsilon_{s,iA}; \varepsilon_{p,iA}\}^T &= R(\bar{e}_X, \bar{s}_{iA})\{\cos\alpha_p, \sin\alpha_p\}^T \\ \varepsilon_{s,iA} &= \varepsilon_{s,iA} t_s^A, \quad \varepsilon_{p,iA} = \varepsilon_{p,iA} t_p^A \\ \{\varepsilon_{s,iB}; \varepsilon_{p,iB}\}^T &= R(\bar{s}_{iA}, \bar{s}_{iB})\{\varepsilon_{s,iA}; \varepsilon_{p,iA}\}^T \\ \varepsilon_{s,iB} &= \varepsilon_{s,iB} t_s^B, \quad \varepsilon_{p,iB} = \varepsilon_{p,iB} t_p^B \\ \{\varepsilon_\Phi^{trans}; \varepsilon_\Psi^{trans}\}^T &= R(\bar{s}_{iB}, \bar{e}_\Phi)\{\varepsilon_{s,iB}; \varepsilon_{p,iB}\}^T. \end{aligned} \quad (13)$$

The unit vectors in the s and p polarization directions for the entrance interface $(\bar{s}_{iA}, \bar{p}_{iA})$ and $(\bar{s}_{eA}, \bar{p}_{eA})$, and for the exit interface $(\bar{s}_{iB}, \bar{p}_{iB})$ and $(\bar{s}_{eB}, \bar{p}_{eB})$ were given by Lock [6]. We formally denote by $R(\bar{u}, \bar{v})$ the plane rotation matrix of angle γ , where $\cos \gamma = (\bar{u} \cdot \bar{v}) / (|\bar{u}| |\bar{v}|)$, and by $t_s^{A(B)}$ and $t_p^{A(B)}$, the Fresnel coefficients for transmission corresponding to the entrance and the exit interfaces, respectively.

2.3.2 Reflected Electric Field

In the case of specular reflection of an arbitrarily polarized plane wave by an arbitrarily oriented axisymmetrical particle, the unit vector of the incident ray \bar{n}_i , the unit vector of the reflected ray \bar{n}_s and the unit normal to the particle surface at the incidence point \bar{n}_A lie in the same plane, i.e. $\bar{n}_A = (\bar{n}_s - \bar{n}_i) / |\bar{n}_s - \bar{n}_i|$. For given values of the scattering angles (Φ_s, Ψ_s) the cosine of the angle Σ between the normal to the surface at the incidence point A and the symmetry axis of the particle is given by

$$\cos \Sigma = \sin \beta \cos(\Phi_s/2) \cos(\Psi_s - \alpha) - \cos \beta \sin(\Phi_s/2). \quad (14)$$

The angular coordinate θ_A can then be obtained by solving the nonlinear equation

$$\theta_A - \arctan\left(\frac{r_A}{r_A}\right) = \Sigma. \quad (15)$$

For a spheroidal particle Eq. (15) simplifies to

$$\theta_A = \arctan\left(\frac{b^2 \tan \Sigma}{a^2}\right) \quad (16)$$

where a and b are the semi-major and the semi-minor axes of the spheroid, respectively.

- (i) The magnitude of the reflected electric field is related to the principal radius of curvature of the particle surface at the incident point

$$\rho_{1A} = \frac{(r_A^2 + r_A^2)^{\frac{3}{2}}}{r_A^2 + 2r_A^2 - r_A \ddot{r}_A}, \quad \rho_{2A} = \frac{r_A \sin \theta_A}{\sin \Sigma} \quad (17)$$

by

$$S_{ref} = \frac{k(\rho_{1A} \rho_{2A})^{0.5}}{2}. \quad (18)$$

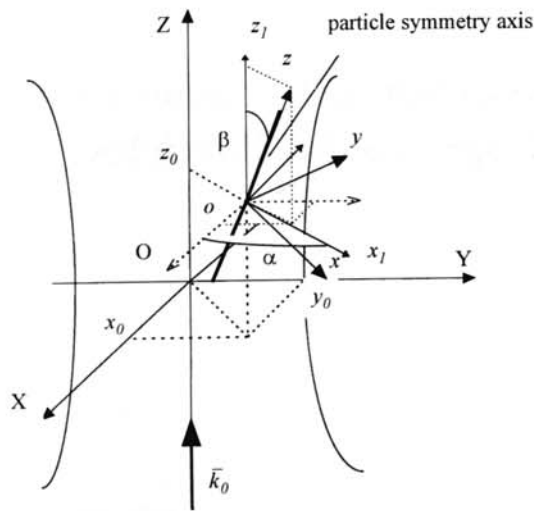


Fig. 1: Beam coordinate system and the particle location system for Gaussian beam incidence.

The spherical coordinates (r, θ, φ) are considered with respect to the particle coordinate system, while (R, Φ, Ψ) represent the set of spherical coordinates in the beam coordinate system.

For a plane wave incidence we put $x_0 = y_0 = z_0 = 0$, $w_0 \rightarrow \infty$ and $r = R$. The other notations remain valid.

2.2 Extended Boundary Condition Method

The extended boundary condition method was developed by Waterman [3] for the solution of electromagnetic scattering by homogeneous non-spherical objects, both conducting and dielectric. The substance of this method is an eigen-based boundary integral equation method weighted by Green's functions of unbounded space.

The scattered field outside the minimum sphere which totally encloses the particle can be written as

$$\vec{E}_{sca}(\vec{r}) = E_0 \sum_{n=1}^{\infty} \sum_{m=-n}^n D_{mn} [f_{mn} \vec{M}_{mn}^3(k\vec{r}) + g_{mn} \vec{N}_{mn}^3(k\vec{r})] \quad (1)$$

where E_0 is the incident electric field strength, D_{mn} is a normalization constant, $\vec{M}_{mn}^3(k\vec{r})$ and $\vec{N}_{mn}^3(k\vec{r})$ are the radiating spherical vector wavefunctions (SVWF) and f_{mn} and g_{mn} are the scattered field coefficients.

The field coefficients of an approximate solution of the scattering boundary value problem f_{mn}^{δ} and g_{mn}^{δ} are related to the incident field coefficients written in the particle coordinate system a_{mn} and b_{mn} by

$$\begin{bmatrix} f_{mn}^{\delta} \\ g_{mn}^{\delta} \end{bmatrix} = -[T] \begin{bmatrix} a_{mn} \\ b_{mn} \end{bmatrix} \quad (2)$$

where $[T]$ is the transition matrix, which contains all the information about the scattered object such as the size, shape and refractive index. The basic technique for the derivation of the $[T]$ matrix was given by Barber and Yeh [4].

Because almost all optical particle sizing counters depend on light scattering of a single particle in one or more laser beams, we consider the most general situation, namely the scattering of Gaussian beams by arbitrarily shaped particles. For a Gaussian beam, the incident field coefficients are computed in an additionally translated coordinate system by using the generalized

localized approximation [8]

$$\begin{pmatrix} a_{m'n} \\ b_{m'n} \end{pmatrix} = (-1)^{m'-1} C_{nm'} K_{nm'} \bar{\Psi}_0^0 e^{ikz_0} \frac{1}{2} \left[e^{i(m'-1)\varphi_0} J_{m'-1} \left(2 \frac{\bar{Q} \rho_0 \rho_n}{w_0^2} \right) \pm e^{i(m'+1)\varphi_0} J_{m'+1} \left(2 \frac{\bar{Q} \rho_0 \rho_n}{w_0^2} \right) \right] \quad (3)$$

where $C_{nm'} = 4i^{n-1} (n + |m'|)! / (n - |m'|)!$ is a normalization constant,

$$K_{nm'} = \begin{cases} (-i)^{|m'|} \frac{i}{(n + 0.5)^{|m'-1|}}, & m' \neq 0 \\ \frac{n(n+1)}{n+0.5}, & m' = 0 \end{cases}$$

is a correction factor and

$$\bar{\Psi}_0^0 = i\bar{Q} e^{-i\bar{Q}\rho_0^2/w_0^2} e^{-i\bar{Q}(n+0.5)^2/(k^2 w_0^2)}$$

$$\rho_n = (n + 0.5)/k, \quad \bar{Q} = 1/(i - 2z_0/l), \quad \rho_0 = (x_0^2 + y_0^2)^{0.5},$$

$$\varphi_0 = \arctg(x_0/y_0).$$

In the particle coordinate system one uses the addition theorem for SVWF under coordinate rotations to obtain

$$\begin{pmatrix} a_{mn} \\ b_{mn} \end{pmatrix} = \sum_{m'=-n}^n R_{m'n}^{mm}(\alpha - \alpha_p, \beta, 0) \begin{pmatrix} a_{m'n} \\ b_{m'n} \end{pmatrix} \quad (4)$$

where $R_{m'n}^{mm}(\alpha, \beta, \gamma)$ is the rotation matrix of Euler angles (α, β, γ) which transforms the spherical vector wavefunctions under successive rotations of the coordinate system.

In the EBCM a single set of bases with expansion coefficients is used to describe the field inside the scatterer. Its solution has poor convergence and even divergent values for dielectric objects with large aspect ratios in the resonance frequency range. To overcome this limitation, various modified versions of the EBCM were derived and implemented in computer codes [10].

2.3 Ray Theory

Ray theory was considered by Lock [5, 6] for an arbitrarily polarized plane wave that is incident upon an arbitrarily oriented spheroid. Our version closely follows the guidelines of this work, but we use a different parametrization of incident rays, which is suitable for axisymmetric particles. In this section we present our algorithm and describe the simplifications which occur for spheroidal particles.

Consider a dielectric axisymmetrical particle of real refractive index m , $m > 1$, whose surface is given in spherical coordinates by $r = r_p(\theta)$. Light is scattered by the particle in the (Φ_s, Ψ_s) direction referenced with respect to the beam coordinate system, while the scattering direction is given by (θ_s, φ_s) in the particle location system. The expressions of transmitted, reflected and diffracted electric fields can be generally written as

$$\vec{E}_{sca}(\Phi_s, \Psi_s) = \frac{iE_0}{kR} e^{ikR} S(\Phi_s, \Psi_s) e^{i\delta(\Phi_s, \Psi_s)} \vec{e}(\Phi_s, \Psi_s) \quad (5)$$

where $S(\Phi_s, \Psi_s)$, $\delta(\Phi_s, \Psi_s)$ and $\vec{e}(\Phi_s, \Psi_s)$ are the magnitude, the phase and the polarization vector of electric-field contributions, respectively.

